J Antimicrob Chemother 2019; **74**: 2617–2625
doi:10.1093/jac/dkz223 Advance Access publication 24 May 2019

Journal of Antimicrobial Chemotherapy

The mechanism of action of pepR, a viral-derived peptide, against *Staphylococcus aureus* biofilms

Sandra N. Pinto[1,2], Susana A. Dias[3], Ana F. Cruz[3], Dalila Mil-Homens[2], Fabio Fernandes[1,2], Javier Valle[4], David Andreu[4], Manuel Prieto[1,2], Miguel A. R. B. Castanho[3], Ana Coutinho[1,2,5]† and Ana Salomé Veiga[3]*†

[1]Centro de Química-Física Molecular e IN, Instituto Superior Técnico, Universidade de Lisboa, Av. Rovisco Pais 1049-001 Lisboa, Portugal; [2]iBB-Institute for Bioengineering and Biosciences, Department of Bioengineering, Instituto Superior Técnico, Universidade de Lisboa, Av. Rovisco Pais 1049-001 Lisboa, Portugal; [3]Instituto de Medicina Molecular, Faculdade de Medicina, Universidade de Lisboa, Av. Prof. Egas Moniz, 1649-028 Lisboa, Portugal; [4]Department of Experimental and Health Sciences, Universitat Pompeu Fabra, Barcelona Biomedical Research Park, 08003 Barcelona, Spain; [5]Departamento de Química e Bioquímica, Faculdade de Ciências, Universidade de Lisboa, Campo Grande 1749-016 Lisboa, Portugal

*Corresponding author. E-mail: aveiga@medicina.ulisboa.pt
†These authors contributed equally to this work.

Received 28 December 2018; returned 12 March 2019; revised 6 April 2019; accepted 23 April 2019

Objectives: To investigate the mechanism of action at the molecular level of pepR, a multifunctional peptide derived from the Dengue virus capsid protein, against *Staphylococcus aureus* biofilms.

Methods: Biofilm mass, metabolic activity and viability were quantified using conventional microbiology techniques, while fluorescence imaging methods, including a real-time calcein release assay, were employed to investigate the kinetics of pepR activity at different biofilm depths.

Results: Using flow cytometry-based assays, we showed that pepR is able to prevent staphylococcal biofilm formation due to a fast killing of planktonic bacteria, which in turn resulted from a peptide-induced increase in the permeability of the bacterial membranes. The activity of pepR against pre-formed biofilms was evaluated through the application of a quantitative live/dead confocal laser scanning microscopy (CLSM) assay. The results show that the bactericidal activity of pepR on pre-formed biofilms is dose and depth dependent. A CLSM-based assay of calcein release from biofilm-embedded bacteria was further developed to indirectly assess the diffusion and membrane permeabilization properties of pepR throughout the biofilm. A slower diffusion and delayed activity of the peptide at deeper layers of the biofilm were quantified.

Conclusions: Overall, our results show that the activity of pepR on pre-formed biofilms is controlled by its diffusion along the biofilm layers, an effect that can be counteracted by an additional administration of peptide. Our study sheds new light on the antibiofilm mechanism of action of antimicrobial peptides, particularly the importance of their diffusion properties through the biofilm matrix on their activity.

Introduction

Bacterial infections are a major human health problem given not only the increasing incidence of drug-resistant bacteria and the decreased search for new antibiotics,[1,2] but also due to the ability of bacteria to form biofilms.[3,4] Bacterial biofilms are surface-associated bacterial communities embedded in a matrix of extracellular polymeric substances (EPSs) that are implicated in the majority of human bacterial infections.[3,5–7] *Staphylococcus aureus*, a Gram-positive bacterium, is a human pathogen commonly involved in biofilm-related infections such as chronic wound infections and medical device-associated infections.[8–10] The treatment of this type of infection is difficult because biofilm-associated bacteria are more tolerant to conventional antibiotics than their planktonic counterparts.[11,12] It is thus urgent to develop novel antimicrobial agents designed to be active against bacterial biofilms.

Antimicrobial peptides (AMPs) are a group of molecules that can be found in all life domains and are known for their activity against Gram-positive and Gram-negative bacteria, viruses and fungi.[13] Although diverse in their amino acid sequences, they are usually small, cationic and amphipathic. AMPs have been

considered potential alternatives to conventional antibiotics[14,15] and, more recently, a promising option against bacterial biofilms.[16,17] Over the years, studies conducted using mostly bacteria in the planktonic state have shown that AMPs have a broad-spectrum, fast bactericidal activity and membrane-targeting mechanism of action[13,15] which makes them good candidates to develop new antibiofilm agents.[18–21] Unlike conventional antibiotics with specific targets, almost exclusively proteins or nucleic acids in metabolically active bacteria, AMPs act mainly through bacterial membrane disruption, which makes them potentially active against slow-growing or non-growing biofilm cells. While the ability of AMPs to act on bacterial biofilms has been addressed,[18,19,21] a thorough and consistent focus on the study of their antibiofilm action at the molecular level is desirable to expand the potential use of AMPs as antibiofilm agents and thus endow anti-infective drug development pipelines.

In the quest for new antimicrobial agents we have recently shown the potential of structural viral proteins, particularly viral capsid proteins, as a source for peptides with antibacterial properties against both Gram-positive and Gram-negative bacteria.[22,23] Interestingly, some of these viral-derived peptides also exhibit cell-penetrating properties that confer potential use on intracellular bacterial targets. One of those peptides, pepR, a synthetic peptide whose sequence corresponds to amino acid residues 67–100 from Dengue virus capsid protein, was reported to be active against Gram-positive and Gram-negative bacteria in the planktonic form.[22] Here, we show that pepR is able to both prevent and act on *S. aureus* biofilms. As such, we have used pepR as a model antibacterial peptide to investigate in detail the molecular mechanism underlying its antibiofilm actions. Using a combination of confocal fluorescence microscopy assays, the spatiotemporal profile of pepR activity against mature *S. aureus* biofilms has been investigated. Our studies highlight the importance of pepR slow diffusion through the extracellular matrix in controlling its killing efficacy at the inner layers of the biofilms.

Materials and methods

Materials and methods are described only briefly here. Further details are provided as Supplementary data (available at *JAC* Online).

pepR synthesis

pepR, LKRWGTIKKSKAINVLRGFRKEIGRMLNILNRRRR-amide,[24] was synthesized using solid-phase 9-fluorenylmethoxycarbonyl (Fmoc) chemistry[25] and purified using HPLC as previously described.[26] pepR stock solutions were prepared in sterile Milli-Q water at 1 or 2 mM and stored at −20°C. The 2-fold serial dilutions of pepR used in the different assays were prepared in Mueller–Hinton broth (MHB), except when otherwise specified.

Bacterial strain and growth conditions

S. aureus strain ATCC 6538 was obtained from the ATCC (Manassas, VA, USA). Bacteria were grown in MHB from BD (Franklin Lakes, NJ, USA) at 37°C. *S. aureus* bacterial biofilms were prepared in tryptic soy broth (TSB), also from BD, containing 0.25% (w/v) glucose (TSBG) for 24 h at 37°C.

Antibacterial and bactericidal activities on planktonic bacterial cells

MIC and MBC were determined using a broth microdilution method[27,28] as previously described.[23]

Inhibition of biofilm formation

Two-fold serial pepR dilutions covering the 0.78–50 μM range were directly added to *S. aureus* suspensions prepared at 1×10^6 cfu/mL in MHB. Untreated bacterial suspensions were used as a control. Each suspension was dispensed into a 96-well microtitre flat-bottomed polystyrene plate (200 μL/well) and incubated at 37°C for 24 h. After incubation, bacterial metabolic activity was assayed using a resazurin reduction fluorometric assay, and the biomass produced was evaluated using a crystal violet (CV) assay.

Effect on established biofilms

S. aureus (1×10^6 cfu/mL) were cultured in TSBG and incubated in 96-well microtitre flat-bottomed polystyrene plates for 24 h at 37°C to allow for biofilm formation. Non-adherent bacteria were then washed out with MHB, and 2-fold serial pepR dilutions (0.78–100 μM) were added to the biofilms for 24 h. Untreated 24 h-pre-formed biofilms were used as a control. The metabolic activity of biofilm cells was determined using a resazurin reduction fluorometric assay, and cell viability was measured using a colony count assay.

Bacterial killing kinetics

The kinetics of the bactericidal effect of pepR on both planktonic and biofilm forms of *S. aureus* was determined using a colony count-based method.[29,30] *S. aureus* suspensions prepared at 5×10^5 cfu/mL on MHB or 24 h-pre-formed biofilms grown in TSBG were treated with increasing concentrations of pepR and incubated for different amounts of time at 37°C (and 200 rpm for the bacterial suspensions). Untreated bacterial suspensions/biofilms prepared under the same experimental conditions were used as a control. At chosen timepoints, the colony count assay was performed. Viable bacteria (in cfu/mL) are reported as a percentage of the untreated control.

Membrane permeabilization of planktonic bacteria

The ability of pepR to induce membrane permeabilization of *S. aureus* in the planktonic form was correlated with the concomitant loss of cell viability by performing a flow cytometric analysis of the SYTOX Green uptake assay in conjunction with a colony count assay as previously described[23] with minor modifications.

Live/dead fluorescence imaging of S. aureus biofilms using confocal laser scanning microscopy (CLSM)

The visualization of the progressive loss of cell viability at different depths of the biofilm-embedded bacteria due to pepR action was achieved by implementing an adapted live/dead assay using SYTO 9 and TO-PRO-3 iodide (Molecular Probes, Eugene, OR, USA) as the green and red fluorescent nucleic acid-binding dyes, respectively, after introducing some modifications to a previously described[31] procedure.

CLSM-based calcein release assay

The ability of pepR to permeabilize the bacterial membrane of *S. aureus* biofilm-embedded cells was evaluated using a CLSM-based calcein release assay adapted from the literature.[32]

Statistical analysis

Data are presented as mean ± standard deviation of three independent experiments performed with three technical replicates each, unless indicated otherwise.

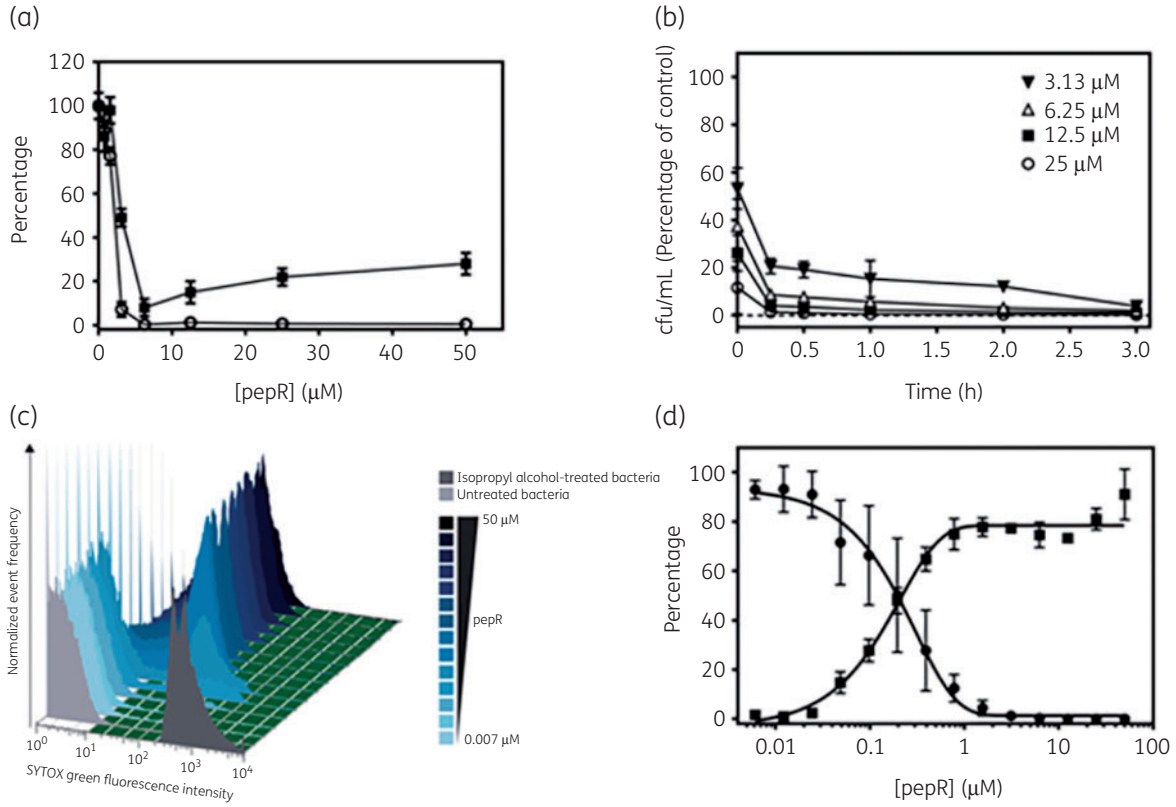

Figure 1. pepR prevents *S. aureus* biofilm formation through a bactericidal activity caused by membrane permeabilization of planktonic cells. (a) pepR inhibits *S. aureus* biofilm formation. Planktonic bacterial cells were incubated for 24 h at 37°C with increasing concentrations of pepR. The metabolic activity and the biofilm biomass of untreated and pepR-treated bacterial cells were evaluated using a resazurin reduction fluorometric kinetic assay (resazurin reduction, % of control, open circles) and a CV binding assay ($\Delta Abs_{590\ nm}$, % of control, filled squares), respectively. The increase in CV staining detected upon increasing the pepR concentration above 6.25 μM was independently confirmed to be due to non-specific binding of CV to the peptide directly adsorbed onto the bare polystyrene microplate surface. (b) pepR induces fast killing kinetics of planktonic *S. aureus*. The time–kill of planktonic bacterial cells by different concentrations of pepR was evaluated using a colony count assay. Viable bacteria (in cfu/mL) are reported as a percentage of the untreated sample. (c and d) The pepR-induced loss of cell viability is inversely correlated with membrane permeabilization of *S. aureus* planktonic cells. (c) Illustrative histogram analysis of the bacterial populations after exposure to variable concentrations of pepR for 1 h that were monitored using a flow cytometric analysis of SYTOX Green uptake by the planktonic bacteria. (d) The fractions of permeabilized bacterial cells (filled squares) and viable bacteria (in cfu/mL, filled circles) are reported as a percentage of the untreated sample.

Results and discussion

pepR is able to both prevent the formation of and act on pre-formed S. aureus biofilms

pepR is a highly cationic, viral-derived peptide known for its antibacterial activity against both Gram-positive and Gram-negative planktonic bacteria. Here, we focused on studying the activity and, most importantly, the mechanism of action of pepR against biofilms of *S. aureus*, one of the most common pathogens responsible for biofilm-related infections.[8,9]pepR was able to prevent the formation of *S. aureus* biofilms (Figure 1a). The biofilm mass, evaluated using a CV assay, after 24 h incubation of planktonic bacteria with the peptide, was maximally reduced at 6.25 μM pepR. This closely matched the parallel drop detected in the metabolic activity of the bacterial cells as measured with a resazurin reduction fluorometric kinetic assay. The inhibition of biofilm formation by pepR was due to a direct effect of the peptide on planktonic *S. aureus*, since pepR displayed high antibacterial activity against the *S. aureus* ATCC 6538 with an MIC of 3.1 μM and an MBC within the 3.1–12.5 μM range. pepR also exhibited a fast killing of planktonic *S. aureus* (Figure 1b), which in turn resulted from the peptide-induced increase in the permeability of the bacterial membranes, as shown using a flow cytometric-based detection of cellular uptake of SYTOX Green dye (Figure 1c and d).

The activity of pepR against biofilms was further evaluated by testing its ability to act on established biofilms as these are more challenging to eradicate. The effect of pepR on 24 h-pre-formed *S. aureus* biofilms was investigated by exposing the biofilms to increasing concentrations of peptide for 24 h. A colony count and resazurin reduction fluorometric kinetic assay (Figure S1) concurrently showed that pepR is able to act on pre-formed biofilms in a dose-dependent fashion, reaching a maximum efficiency at ~50 μM (Figure 2a). As expected, the pepR-induced killing kinetics of the biofilm-embedded cells were slower when compared with the planktonic bacteria, reaching a plateau after 2 h incubation of the pre-formed biofilm with pepR, as exemplified in Figure 2(b) for 25 and 50 μM pepR. In fact, the reduction in the percentage of viable/live cells produced upon increasing the concentration of

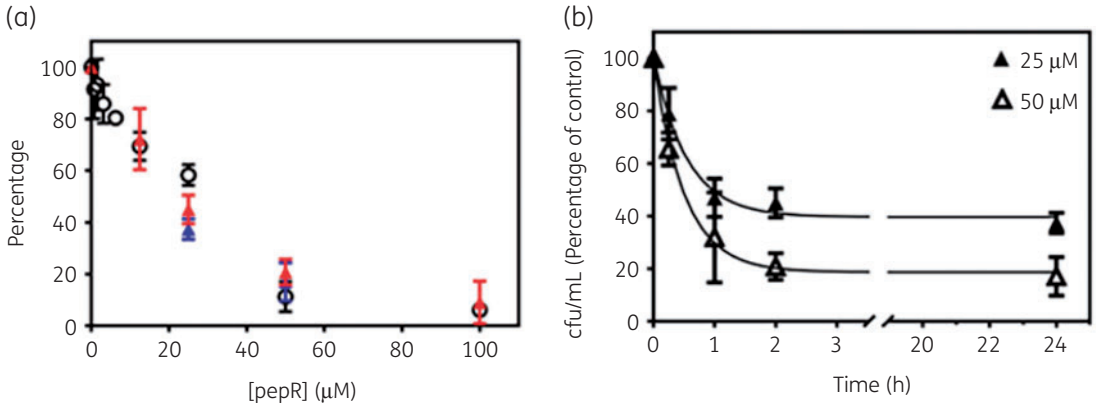

Figure 2. pepR acts on pre-formed *S. aureus* biofilms in a concentration- and time-dependent manner. (a) Effect of pepR on the viability of *S. aureus* biofilm-associated cells. 24 h-pre-formed biofilms were incubated for 2 h or 24 h at 37°C with increasing concentrations of pepR. The metabolic activity of untreated and pepR-treated bacterial cells for 24 h was measured using a resazurin reduction fluorometric kinetic assay (resazurin reduction, % of control, open circles); bacterial viability after 2 h (red filled triangles) or 24 h (blue filled triangles) pepR treatment was also evaluated using a colony count assay (cfu/mL, % of control). (b) The time–kill of biofilm-embedded bacteria induced by 25 and 50 μM pepR was evaluated using a colony count assay (cfu/mL, % of control).

pepR was found to be very similar after 2 or 24 h treatment for all the concentrations of pepR tested (Figure 2a).

The bactericidal activity of pepR on pre-formed S. aureus biofilms is depth dependent

To directly visualize and quantify the bactericidal activity of pepR on 24 h-pre-formed *S. aureus* biofilms at different biofilm depths, we performed a live/dead CLSM-based study using SYTO 9 and TO-PRO-3 iodide as the nucleic acid-binding dyes. SYTO 9 is a membrane-permeable dye that stains all bacteria green (with intact and damaged membranes) in a population, whereas TO-PRO-3 iodide only penetrates and stains red any bacteria with damaged membranes.[31,33]

Representative CLSM images obtained at an inner layer (z=1.5 μm, z being the distance from the surface of the glass slide) of 24 h-pre-formed biofilms which were untreated or treated with 25 or 50 μM pepR for 2 h, and then sequentially stained with SYTO 9 and TO-PRO-3 iodide, are presented in Figure 3(a). Treatment of pre-formed biofilms with increasing concentrations of pepR produced a clear increase in the red-stained circular aggregates with high fluorescence intensity (Figure S2) and a concomitant reduction of bacteria stained with SYTO 9 (left panels of Figure 3a, SYTO 9 and TO-PRO-3 iodide, *x*–*y* plane images). This double opposing effect registered in the green and red channels of the CLSM *x*–*y* plane images confirms the ability of pepR to kill biofilm-associated bacteria through the disruption of their membranes. Quantification of the degree of co-localization between the two fluorescent dyes was achieved by colour scatter plots and calculation of the Pearson's correlation coefficient (PCC).[34] As shown in the central panels of Figure 3(a) (overlay, *x*–*y*), their corresponding scatter plots suggest that TO-PRO-3 iodide enters the biofilm-embedded bacteria upon pepR-induced membrane damage, partially displacing the intracellular DNA (iDNA)-bound SYTO 9 dye due to a competition effect. This causes the membrane-compromised bacteria to appear orange in both the *x*–*y* and *x*–*z* overlay plots (Figure 3a). The average PCC value for the untreated and 50 μM pepR-treated double-stained biofilms at z=1.5 μm were PCC=−0.06±0.16 and PCC = 0.78±0.04, respectively (Figure 3b), which essentially correspond to an observation field with all the bacteria with either an intact or compromised plasma membrane, respectively. Interestingly, the PCC values obtained at this biofilm depth for the double-stained pre-formed biofilms treated with the intermediate concentration of 25 μM pepR presented a bimodal distribution, with the observation fields containing either predominantly membrane-intact (PCC=−0.03±0.15) or membrane-compromised bacteria (PCC=0.59±0.12). As we move away from the coverslip [i.e. from an inner (z=1.5 μm) to an outer (z=10.5 μm) biofilm layer] (Figure S3), the cellular density of the untreated biofilms becomes more rarefied and their corresponding PCC value slightly increases from PCC(z=1.5 μm)=−0.09±0.14 to PCC(z=7.5 μm)=0.07±0.11, and finally to PCC(z=10.5 μm) =0.16±0.09 (Figure 3c). This result most probably reflects the simultaneous binding of both fluorescent dyes to the extracellular DNA (eDNA), which is more abundant at the outer compared with the inner biofilm layer. Interestingly, an analogous analysis of the biofilms treated for 2 h with 25 μM pepR reveals that the bimodal distribution of PCC values detected at z=1.5 μm (PCC=0.06±0.10 and PCC=0.51±0.09) progressively shifts to an unimodal distribution with PCC=0.63±0.17 at z=10.5 μm (Figure 3c), revealing that the bacterial membranes of the biofilm-embedded bacteria at the periphery of the biofilm are more uniformly and reproducibly compromised by pepR action compared with an inner layer.

pepR antibiofilm properties are controlled by its diffusion along the biofilm matrix

The above data strongly suggest that the biofilm matrix is acting as a barrier that reduces/slows down the penetration of pepR, with a consequent decrease in activity at the more deeply biofilm-embedded bacterial cells. To obtain a clearer picture of the spatio-temporal profile of pepR activity, we next sought to investigate the time dependence of its action at different biofilm depths. A real-time CLSM assay of calcein release from CAM-pre-loaded 24 h-pre-formed *S. aureus* biofilms was developed to indirectly assess the diffusion and membrane permeabilization properties of pepR

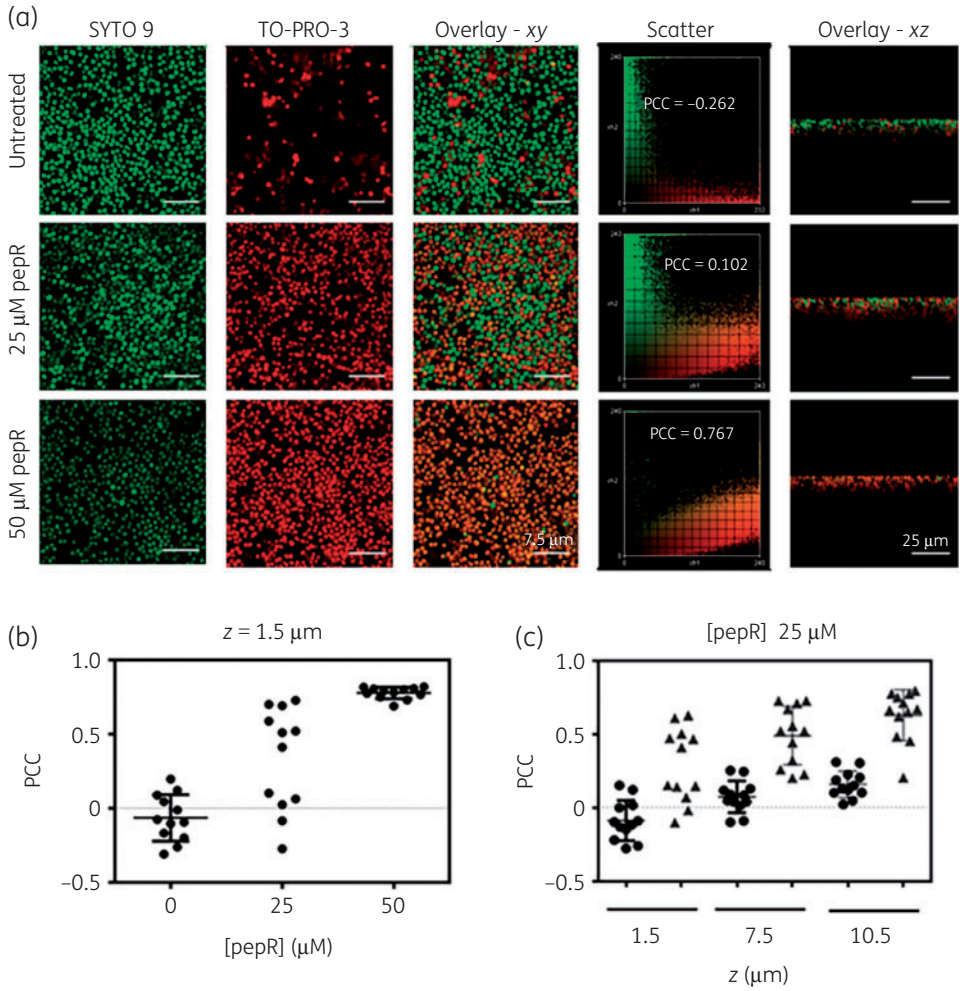

Figure 3. CLSM-based analysis of the influence of pepR concentration and biofilm depth on the pepR-induced decrease in the viability of biofilm-embedded bacteria. (a) Representative CLSM images of 24 h-pre-formed biofilms untreated and pepR treated for 2 h; the biofilms were stained with the nucleic acid-binding dyes SYTO 9 and TO-PRO-3 iodide. SYTO 9 passively diffuses across intact cell membranes and binds to the iDNA; TO-PRO-3 iodide is excluded from cells with structurally intact membranes and can only bind the iDNA of membrane-compromised bacteria. The left panels correspond to *x*–*y* plane images taken at the inner layer of *S. aureus* stained biofilms (z=1.5 μm). The overlay of the green and red channels from the *x*–*y* and *x*–*z* orthogonal plane images is presented in the central and right panels, respectively. The extent of fluorophore co-localization can be evaluated from the central scatter plots; the PCC was quantified using the WCIF ImageJ software. (b and c) The degree of co-localization between SYTO 9 and TO-PRO-3 iodide varies with (b) the pepR concentration used at an inner biofilm layer (z=1.5 μm) and (c) the biofilm depth, *z*, in the presence of 25 μM pepR [untreated (filled circles) and pepR-treated (filled triangles) pre-formed *S. aureus* biofilms].

throughout the biofilm over time[32] (Figure 4a). CAM is a non-fluorescent calcein derivative that passively diffuses across plasma membranes; once inside the cytoplasm, CAM is hydrolysed by cytoplasmic esterases, releasing highly fluorescent calcein.[35] Due to its anionic character, calcein is retained in live cells with intact membranes;[32,35] damage to membrane integrity induces calcein release from the bacterial cells and its subsequent dilution into the extracellular media, causing a decrease in the fluorescence intensity. The corresponding kinetics (cellular uptake and leakage of the dye, respectively) from biofilm-embedded bacteria can therefore be monitored by measuring the relative changes in the fluorescence intensity of calcein over time at different biofilm depths using CLSM.

Illustrative time-lapsed *x*–*z* vertical slice images of 24 h-pre-formed *S. aureus* biofilms pre-loaded with CAM during an incubation period of 3 h and then left untreated or treated with pepR at 50 μM for 2 h are presented in Figure 4(b). A first quantitative analysis of these images was performed by evaluating the relative changes over time in the average fluorescence emission intensity from a rectangular region of interest (ROI) encompassing the calcein-stained pre-formed biofilms. Figure 4(c) shows that pepR induced a monoexponential decay of the average calcein fluorescence emission intensity over the 2 h incubation with $t_{1/2}$=23 min. On the other hand, the average fluorescence emission intensity of calcein-pre-loaded biofilms left untreated slightly increased during the same time period, possibly due to residual CAM hydrolysis by the intact biofilm-embedded bacteria. This result rules out that significant spontaneous calcein leakage is occurring during the assay or that calcein is cytotoxic at the concentration used.

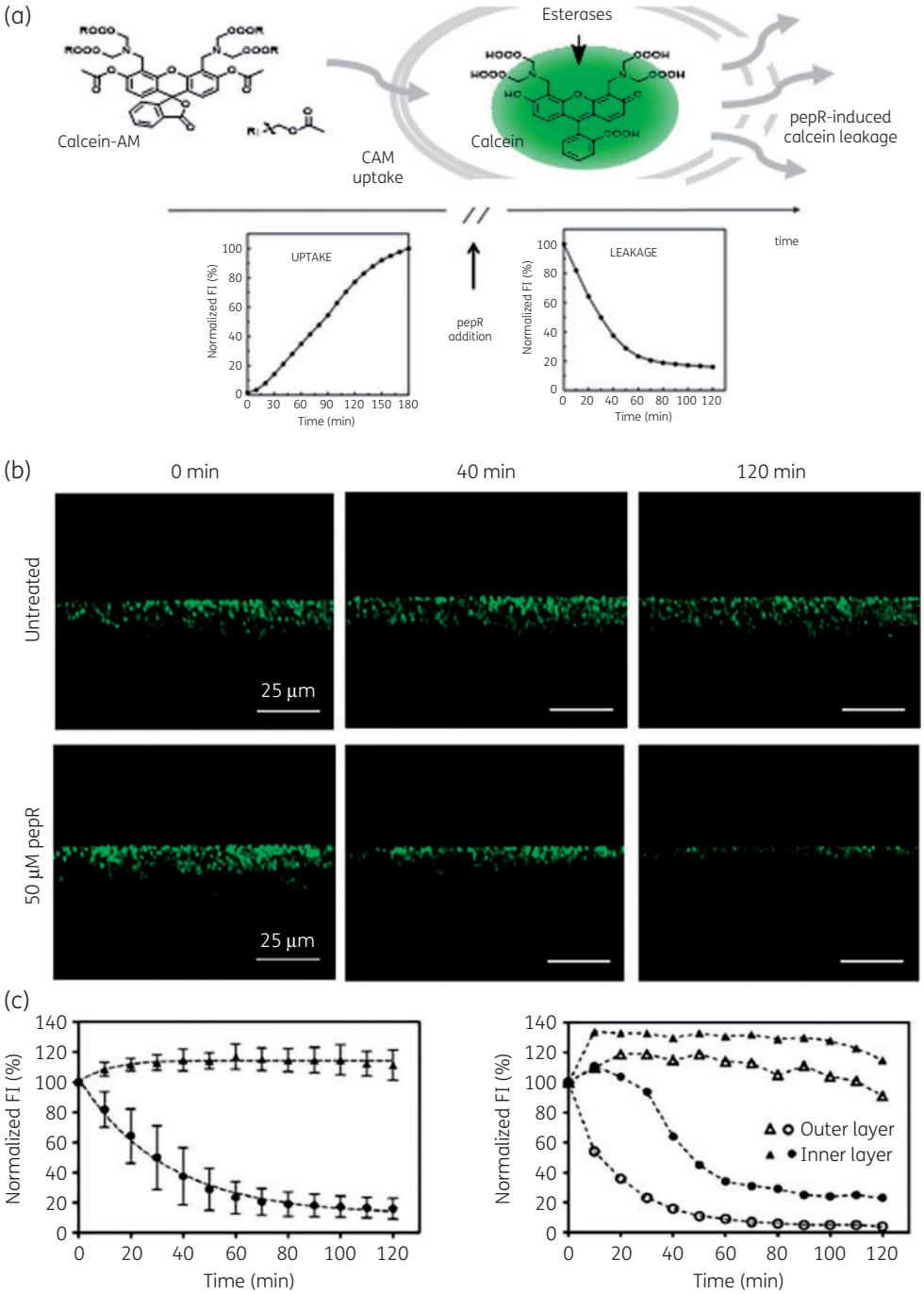

Figure 4. Time-lapsed CLSM-based imaging study of the pepR-induced calcein release from biofilm-embedded bacteria. (a) Top panel: the non-fluorescent derivative of calcein, CAM, can be taken up by the cells through passive diffusion across their plasma membranes; once inside the cytoplasm, CAM is readily hydrolysed by cytoplasmic esterases, releasing calcein, a highly fluorescent compound. The pepR-induced increase in cell membrane permeability causes the subsequent release and dilution of calcein in the medium. Bottom panels: representative calcein uptake (left panel) and release (right panel) kinetics for 24 h-pre-formed *S. aureus* biofilms incubated with CAM over 3 h and then treated with pepR for an additional period of 2 h. (b) Illustrative time-lapsed CLSM images of calcein release from untreated and pepR-treated 24 h-pre-formed biofilms. Orthogonal views to the *S. aureus* biofilms surface (*xzy* sections) were taken every 10 min for a total of 2 h. (c) Relative changes in the average calcein fluorescence intensity (FI) from a pre-defined rectangular ROI encompassing the untreated (filled triangles) and pepR-treated (filled circles) calcein-stained biofilms over time. The relative FI values are the mean ± SD of five independent experiments. A mono-exponential decay by non-linear regression (solid line) was fitted to the data obtained for the pepR-treated samples. (d) Illustrative influence of biofilm depth on the calcein release kinetics from untreated (triangles) and pepR-treated (circles) calcein-stained pre-formed biofilms from an inner (z=3 µm, filled symbols) and outer (z=10 µm, open symbols) biofilm layer, respectively.

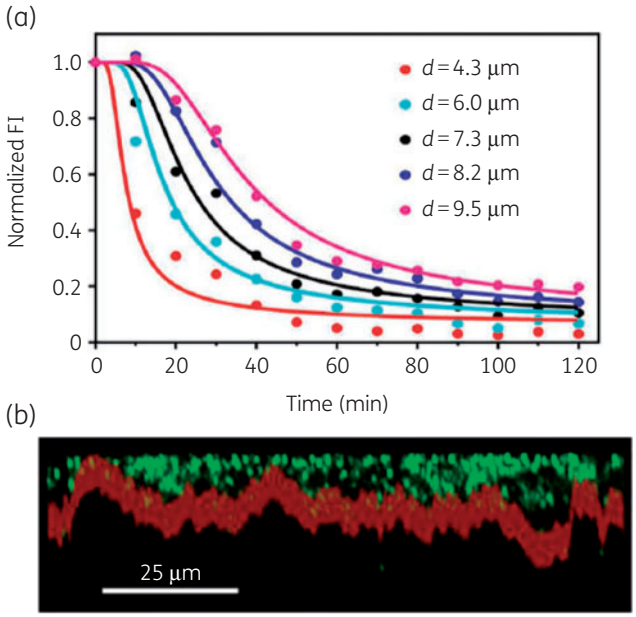

Figure 5. pepR action on biofilm-embedded bacteria is strongly diffusion controlled. (a) Representative data illustrating the relative changes in the fluorescence emission intensity of calcein over time and biofilm distance from the interface after pepR addition to a pre-formed calcein-stained biofilm. Supplementary Equation 4 was used to globally fit the data obtained at 17 different biofilm distances, *d*, from the interface. Solid lines illustrate the global best fit solution to five of these data sets, from which $D=4.5\times10^{-3}$ μm^2 s^{-1} and $K_{app}=4.1\times10^{-1}$ μM^{-1} were retrieved. (b) Illustrative 2D image of a calcein-loaded biofilm (pseudo-coloured in green). The red shaded area highlights the peripheral biofilm area that was analysed using Supplementary Equation 4. The roughness of the biofilm interface was taken into account in this analysis as shown here.

A more detailed analysis of the data allowed identification of different spatiotemporal patterns of fluorescence loss when the calcein-pre-loaded biofilms were exposed to pepR (Figure S4). The data obtained at two representative biofilm depths are plotted in Figure 4(d). This figure shows that at a biofilm depth close to the interface between the biofilm and the bulk fluid ($z=10$ μm), pepR caused a relatively fast and complete loss of calcein fluorescence emission intensity. However, at an inner layer of the biofilm nearer the coverslip surface ($z=3$ μm), a clear lag time of ∼30 min was detected before the relative change in the fluorescence signal from calcein started to decrease towards a limiting value of ∼20% after a 2 h incubation. These results can be ascribed to the progressive diffusion/binding of pepR through the biofilm matrix. In order to obtain an estimate for the diffusion coefficient of the peptide, a simple model describing the time and depth dependence of the diffusion of pepR throughout the biofilm matrix was derived by assuming that the calcein fluorescence emission intensity tends to zero over space and time (Supplementary Equation 4 in the Supplementary data). As illustrated in Figure 5(a), this model adequately fitted the experimental data obtained from the peripheral biofilm layers [from $d=3.5$ μm to $d=11$ μm (Figure 5b), where *d* is now the distance from the biofilm interface to the aqueous solution], and the globally fitted diffusion coefficient obtained for pepR was $D_{biofilm}=4.5\times10^{-3}$ μm^2 s^{-1}. This value is several orders of magnitude lower than the expected diffusion coefficient for a random-coiled peptide with a molecular weight of 4.3 kDa that is freely diffusing in aqueous solution at room temperature ($D_{solution}=140$ μm^2 s^{-1},[36] and is typical of large charged molecules diffusing in dense media such as the cell nucleus.[37] Such a slow diffusion of pepR can be ascribed to the high viscosity of the EPS matrix[38] and the establishment of electrostatic interactions between the highly cationic peptide (net charge +13 at physiological pH) and the negatively charged polyelectrolytes of the EPS matrix.[39] Other effects, such as 'corralling' and the presence of obstacles hindering free diffusion,[40,41] may also contribute to slow molecular progression of pepR within the biofilm. For comparison, a similar although not so pronounced effect has already been described for the smaller fluorescently labelled antibiotic vancomycin-BODIPY (∼1.7 kDa and net charge 0.7 at physiological pH), as its diffusion was found to be much slower through a biofilm matrix compared with in aqueous solution ($D_{biofilm}=0.5\pm0.2$ μm^2 s^{-1} versus $D_{solution}=180\pm60$ μm^2 s^{-1}).[42]

pepR progressive diffusion into the extracellular matrix controls its availability and antibiofilm activity

The data presented in Figure 2 show that ∼15%–20% of biofilm-embedded bacteria survived a single peptide treatment, after 24 h incubation. On the other hand, both the live/dead and the calcein release CLSM-based studies revealed that the pepR-induced increase in membrane permeability is strongly dependent on the biofilm depth. Two main factors may be responsible for these effects: (i) the majority of pepR added in a single dose interacts with the biofilm matrix components, reducing the amount of free peptide available to reach the inner layers of the biofilm; or (ii) a subpopulation of bacteria resistant to peptide treatment is present at the inner layers of the biofilm. In the first case, we reasoned that if pepR interacts with the biofilm matrix components, nearly reaching its saturation limit after the first treatment, then the addition of a second dose of peptide should allow this effect to be overcome due to the increased availability of free peptide. To test this hypothesis, we performed an experiment where 24 h-pre-formed *S. aureus* biofilms were first treated for 24 h with 50 μM pepR (Figure 6, left); the pre-treated biofilms were then exposed to a second peptide dose of 25 or 50 μM. The results revealed a pronounced increase in the killing efficacy of the peptide with the second dose, as the percentage of bacterial survival decreased from 20% (Figure 6, left) with the first treatment to 3%–4% with the second treatment (Figure 6, middle left). To further validate these results and discard the second hypothesis, additional experiments were performed. First, 24 h-pre-formed *S. aureus* biofilms were treated for 24 h with 50 μM pepR. Then, these pre-treated biofilm cells were washed, re-suspended (∼10^8 cfu/mL) and exposed to a second peptide dose of 25 or 50 μM. The results showed a percentage of bacterial survival of 0.5%–1% (Figure 6, middle right), which is similar to what was obtained when the cells in the biofilm form were directly treated sequentially with two doses of pepR (Figure 6, middle left). In addition, we found that the killing efficacy of pepR was very similar when the same concentrations of the peptide were directly added to a high bacteria inoculum (bacteria in planktonic form that have not gone through a biofilm stage) (Figure 6, right). Altogether, these results rule out the possibility that the biofilm-embedded bacteria at the inner

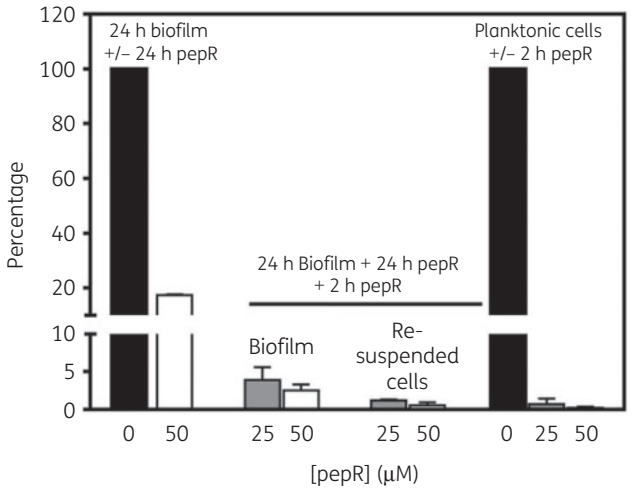

Figure 6. pepR redosing is necessary to achieve a higher killing efficacy on *S. aureus* established biofilms. 24 h-pre-formed *S. aureus* biofilms (left columns) were left untreated or treated with 50 μM pepR for 24 h. The peptide was removed and the biofilms were further exposed to 25 or 50 μM pepR for an additional period of 2 h (middle columns). Additionally, re-suspended bacteria (middle columns) obtained after disrupting 24 h pepR-treated biofilms were treated again with 25 or 50 μM for 2 h. Control planktonic (right columns) bacteria (high inoculum, 10^8 cfu/mL) were left untreated or treated with 25 or 50 μM pepR for 2 h. In each case, bacterial viability was evaluated using a colony count assay (cfu/mL, % of control).

biofilm layers are adaptively resistant to peptide treatment, and strongly support the conclusion that there is a graded activity of pepR along distinct biofilm layers, which in turn is caused by the development of a concentration gradient of pepR along its depth due to its strong interaction with matrix components. Once pepR interaction with the extracellular matrix is close to saturation, the administration of a new peptide dose results in a pronounced increase in its killing efficacy because the peptide is now able to slowly reach the inner biofilm layers at a concentration above the threshold controlling the pepR-induced increase in membrane permeability.

Taken together, these results support the conclusion that biofilm treatment with sequential doses of an AMP is a valid strategy to increase its overall killing efficacy. Another useful approach already proposed in the literature involves using AMPs in combination with other antibacterial agents to produce a synergistic effect, and therefore improve their activity against biofilms.[43] These could include the use of enzymes capable of disrupting the extracellular matrix and therefore facilitating AMP activity against biofilm-associated cells.[44,45]

Conclusions

We have used pepR, a peptide derived from the Dengue virus capsid protein, as a model to study in detail the antibiofilm action of an antibacterial peptide at the molecular level. Importantly, we showed that pepR has dual activity, acting both as an antimicrobial and as an antibiofilm molecule. pepR was found to exert a fast bactericidal activity on planktonic *S. aureus* cells, thus preventing biofilm formation. On the other hand, the spatiotemporal patterns of pepR-induced killing of biofilm-embedded bacteria showed that pepR activity on pre-formed biofilms was strongly diffusion controlled, causing delayed killing at the inner biofilm layers. pepR diffusion through the biofilm matrix is possibly dictated by the high viscosity of the medium, 'corralling' and the establishment of electrostatic interactions with the anionic matrix. Biofilm treatment with sequential doses of pepR resulted in more efficient killing of biofilm cells, highlighting that the inner biofilm layers do not consist of bacteria adaptively resistant to peptide treatment. Taken together, these results shed light on the effect of the biofilm matrix on the diffusion of antibacterial molecules and its influence on their activity.

Funding

This work was supported by the Fundação para a Ciência e a Tecnologia (FCT)/Ministério da Ciência, Tecnologia e Ensino Superior (MCTES) (projects PTDC/QEQ-MED/4412/2014, FAPESP/20107/2014, SAICTPAC/0019/2015, PPBI-POCI-01-0145-FEDER-022122); by the Spanish Ministry of Economy and Competitiveness (MINECO) (grant AGL2014-5239-C2-2R); and by the Marie Skłodowska-Curie Research and Innovation Staff Exchange (grant H2020-MSCA-RISE-2014–644167). We also acknowledge project UID/BIM/50005/2019, funded by FCT/MCTES through Fundos do Orçamento de Estado. S. N. P., S. A. D., A. F. C. and D. M.-H. are the recipients of fellowships from the FCT (SFRH/BPD/92409/2013, PD/BD/114425/2016, PD/BD/136866/2018 and SFRH/BPD/91831/2012, respectively). A. S. V. and F. F. are FCT Researchers (IF/00803/2012 and IF/00386/2015, respectively).

Transparency declarations

None to declare.

Supplementary data

Supplementary data, including Methods and Figures S1–S4, are available at *JAC* Online.

References

1 Klein EY, Van Boeckel TP, Martinez EM *et al*. Global increase and geographic convergence in antibiotic consumption between 2000 and 2015. *Proc Natl Acad Sci USA* 2018; **115**: E3463–70.

2 Coates AR, Halls G, Hu Y. Novel classes of antibiotics or more of the same? *Br J Pharmacol* 2011; **163**: 184–94.

3 Costerton JW, Stewart PS, Greenberg EP. Bacterial biofilms: a common cause of persistent infections. *Science* 1999; **284**: 1318–22.

4 Flemming HC, Wingender J, Szewzyk U *et al*. Biofilms: an emergent form of bacterial life. *Nat Rev Microbiol* 2016; **14**: 563–75.

5 Hall-Stoodley L, Costerton JW, Stoodley P. Bacterial biofilms: from the natural environment to infectious diseases. *Nat Rev Microbiol* 2004; **2**: 95–108.

6 Romling U, Balsalobre C. Biofilm infections, their resilience to therapy and innovative treatment strategies. *J Intern Med* 2012; **272**: 541–61.

7 Del Pozo JL. Biofilm-related disease. *Expert Rev Anti Infect Ther* 2018; **16**: 51–65.

8 Archer NK, Mazaitis MJ, Costerton JW *et al*. *Staphylococcus aureus* biofilms: properties, regulation, and roles in human disease. *Virulence* 2011; **2**: 445–59.

9 Bhattacharya M, Wozniak DJ, Stoodley P *et al*. Prevention and treatment of *Staphylococcus aureus* biofilms. *Expert Rev Anti Infect Ther* 2015; **13**: 1499–516.

10 Hall-Stoodley L, Stoodley P, Kathju S *et al*. Towards diagnostic guidelines for biofilm-associated infections. *FEMS Immunol Med Microbiol* 2012; **65**: 127–45.

11 Brown MR, Allison DG, Gilbert P. Resistance of bacterial biofilms to antibiotics: a growth-rate related effect? *J Antimicrob Chemother* 1988; **22**: 777–80.

12 Davies D. Understanding biofilm resistance to antibacterial agents. *Nat Rev Drug Discov* 2003; **2**: 114–22.

13 Epand RM, Vogel HJ. Diversity of antimicrobial peptides and their mechanisms of action. *Biochim Biophys Acta* 1999; **1462**: 11–28.

14 Baltzer SA, Brown MH. Antimicrobial peptides: promising alternatives to conventional antibiotics. *J Mol Microbiol Biotechnol* 2011; **20**: 228–35.

15 Mahlapuu M, Hakansson J, Ringstad L *et al*. Antimicrobial peptides: an emerging category of therapeutic agents. *Front Cell Infect Microbiol* 2016; **6**: 194.

16 Di Luca M, Maccari G, Nifosi R. Treatment of microbial biofilms in the post-antibiotic era: prophylactic and therapeutic use of antimicrobial peptides and their design by bioinformatics tools. *Pathog Dis* 2014; **70**: 257–70.

17 Strempel N, Strehmel J, Overhage J. Potential application of antimicrobial peptides in the treatment of bacterial biofilm infections. *Curr Pharm Des* 2015; **21**: 67–84.

18 Seo MD, Won HS, Kim JH *et al*. Antimicrobial peptides for therapeutic applications: a review. *Molecules* 2012; **17**: 12276–86.

19 Fritsche TR, Rhomberg PR, Sader HS *et al*. Antimicrobial activity of omiganan pentahydrochloride against contemporary fungal pathogens responsible for catheter-associated infections. *Antimicrob Agents Chemother* 2008; **52**: 1187–9.

20 Segev-Zarko L, Saar-Dover R, Brumfeld V *et al*. Mechanisms of biofilm inhibition and degradation by antimicrobial peptides. *Biochem J* 2015; **468**: 259–70.

21 Chennupati SK, Chiu AG, Tamashiro E *et al*. Effects of an LL-37-derived antimicrobial peptide in an animal model of biofilm *Pseudomonas sinusitis*. *Am J Rhinol Allergy* 2009; **23**: 46–51.

22 Freire JM, Almeida DS, Flores L *et al*. Mining viral proteins for antimicrobial and cell-penetrating drug delivery peptides. *Bioinformatics* 2015; **31**: 2252–6.

23 Dias SA, Freire JM, Perez-Peinado C *et al*. New potent membrane-targeting antibacterial peptides from viral capsid proteins. *Front Microbiol* 2017; **8**: 775.

24 Freire JM, Veiga AS, Conceicao TM *et al*. Intracellular nucleic acid delivery by the supercharged dengue virus capsid protein. *PLoS One* 2013; **8**: e81450.

25 Fields GB, Noble RL. Solid phase peptide synthesis utilizing 9-fluorenylmethoxycarbonyl amino acids. *Int J Pept Protein Res* 1990; **35**: 161–214.

26 Freire JM, Veiga AS, de la Torre BG *et al*. Quantifying molecular partition of cell-penetrating peptide–cargo supramolecular complexes into lipid membranes: optimizing peptide-based drug delivery systems. *J Pept Sci* 2013; **19**: 182–9.

27 Pankey GA, Sabath LD. Clinical relevance of bacteriostatic versus bactericidal mechanisms of action in the treatment of Gram-positive bacterial infections. *Clin Infect Dis* 2004; **38**: 864–70.

28 Wiegand I, Hilpert K, Hancock RE. Agar and broth dilution methods to determine the minimal inhibitory concentration (MIC) of antimicrobial substances. *Nat Protoc* 2008; **3**: 163–75.

29 Garcia-Armesto MR, Prieto M, Garcia-Lopez ML *et al*. Modern microbiological methods for foods: colony count and direct count methods. A review. *Microbiologia* 1993; **9**: 1–13.

30 Mangoni ML, Papo N, Barra D *et al*. Effects of the antimicrobial peptide temporin L on cell morphology, membrane permeability and viability of *Escherichia coli*. *Biochem J* 2004; **380**: 859–65.

31 Stiefel P, Schmidt-Emrich S, Maniura-Weber K *et al*. Critical aspects of using bacterial cell viability assays with the fluorophores SYTO9 and propidium iodide. *BMC Microbiol* 2015; **15**: 36.

32 Davison WM, Pitts B, Stewart PS. Spatial and temporal patterns of biocide action against *Staphylococcus epidermidis* biofilms. *Antimicrob Agents Chemother* 2010; **54**: 2920–7.

33 Van Hooijdonk CA, Glade CP, Van Erp PE. TO-PRO-3 iodide: a novel HeNe laser-excitable DNA stain as an alternative for propidium iodide in multiparameter flow cytometry. *Cytometry* 1994; **17**: 185–9.

34 Dunn KW, Kamocka MM, McDonald JH. A practical guide to evaluating colocalization in biological microscopy. *Am J Physiol Cell Physiol* 2011; **300**: C723–42.

35 Miles FL, Lynch JE, Sikes RA. Cell-based assays using calcein acetoxymethyl ester show variation in fluorescence with treatment conditions. *J Biol Methods* 2015; **2**: e29.

36 Danielsson J, Jarvet J, Damberg P *et al*. Translational diffusion measured by PFG-NMR on full length and fragments of the Alzheimer Aß(1–40) peptide. Determination of hydrodynamic radii of random coil peptides of varying length. *Magn Reson Chem* 2002; **40**: S89–97.

37 Oeffinger M, Zenklusen D. To the pore and through the pore: a story of mRNA export kinetics. *Biochim Biophys Acta* 2012; **1819**: 494–506.

38 Jefferson KK, Goldmann DA, Pier GB. Use of confocal microscopy to analyze the rate of vancomycin penetration through *Staphylococcus aureus* biofilms. *Antimicrob. Agents Chemother* 2005; **49**: 2467–73.

39 Zhang Z, Nadezhina E, Wilkinson KJ. Quantifying diffusion in a biofilm of *Streptococcus mutans*. *Antimicrob Agents Chemother* 2011; **55**: 1075–81.

40 Veith R, Sorkalla T, Baumgart E *et al*. Balbiani ring mRNPs diffuse through and bind to clusters of large intranuclear molecular structures. *Biophys J* 2010; **99**: 2676–85.

41 Siebrasse JP, Veith R, Dobay A *et al*. Discontinuous movement of mRNP particles in nucleoplasmic regions devoid of chromatin. *Proc Natl Acad Sci USA* 2008; **105**: 20291–6.

42 Daddi OS, Briandet R, Fontaine-Aupart MP *et al*. Correlative time-resolved fluorescence microscopy to assess antibiotic diffusion-reaction in biofilms. *Antimicrob Agents Chemother* 2012; **56**: 3349–58.

43 Grassi L, Maisetta G, Esin S *et al*. Combination strategies to enhance the efficacy of antimicrobial peptides against bacterial biofilms. *Front Microbiol* 2017; **8**: 2409.

44 Gawande PV, Leung KP, Madhyastha S. Antibiofilm and antimicrobial efficacy of DispersinB(R)-KSL-W peptide-based wound gel against chronic wound infection associated bacteria. *Curr Microbiol* 2014; **68**: 635–41.

45 Jones EA, McGillivary G, Bakaletz LO. Extracellular DNA within a nontypeable *Haemophilus influenzae*-induced biofilm binds human beta defensin-3 and reduces its antimicrobial activity. *J Innate Immun* 2013; **5**: 24–38.